Lowest n,π^* Triplet State of 2-Cyclopenten-1-one: Cavity Ringdown Absorption Spectrum and Ring-Bending Potential-Energy Function†

Nathan R. Pillsbury,‡ Jaebum Choo,§ Jaan Laane,|| and Stephen Drucker*,‡

Department of Chemistry, University of Wisconsin−Eau Claire, Eau Claire, Wisconsin 54702-4004, Department of Chemistry, Hanyang University, Ansan 425-791, Korea, and Department of Chemistry, Texas A&M University, College Station, Texas 77843-3255

Received: April 16, 2003; In Final Form: July 10, 2003

The room-temperature cavity ringdown absorption spectra of 2-cyclopenten-1-one (2CP) and deuterated derivatives were recorded near 385 nm. The very weak ($\epsilon < 1$ M^{-1} cm^{-1}) band system in this region is due to the $T_1 \leftarrow S_0$ electronic transition, where T_1 is the lowest-energy $^3(n,\pi^*)$ state. The origin band was observed at 25 963.55(7) cm^{-1} for the undeuterated molecule and at 25 959.38(7) and 25 956.18(7) cm^{-1} for 2CP-5-d_1 and 2CP-5,5-d_2, respectively. For the -d_0 isotopomer, about 50 vibronic transitions have been assigned in a region from −500 to +500 cm^{-1} relative to the origin band. Nearly every corresponding assignment was made in the -d_2 spectrum. Several excited-state fundamentals have been determined for the d_0/d_2 isotopomers, including ring-twisting (ν'_{29} = 238.9/227.8 cm^{-1}), out-of-plane carbonyl deformation (ν'_{28} = 431.8/420.3 cm^{-1}), and in-plane carbonyl deformation (ν'_{19} = 346.2/330.2 cm^{-1}). The ring-bending (ν'_{30}) levels for the T_1 state were determined to be at 36.5, 118.9, 213.7, 324.5, and 446.4 cm^{-1} for the undeuterated molecule. These drop to 29.7, 101.9, 184.8, 280.5, and 385.6 cm^{-1} for the -d_2 molecule. A potential-energy function of the form $V = ax^4 + bx^2$ was fit to the ring-bending levels for each isotopic species. The fitting procedure utilized a kinetic-energy expansion that was calculated based on the structure obtained for the triplet state from density functional calculations. The barrier to planarity, determined from the best-fitting potential-energy functions for the -d_0, -d_1, and -d_2 species, ranges from 42.0 to 43.5 cm^{-1}. In the T_1 state, electron repulsion resulting from the spin flip favors nonplanarity. The S_0 and S_1 states have planar structures that are stabilized by conjugation.

Introduction

Molecular triplet states often mediate photochemical events. Characterization of triplet potential-energy surfaces is therefore an important goal. This goal has fueled the ongoing effort within the quantum chemistry community to develop efficient computational techniques for treating excited states (notably triplets) as accurately as the ground state.[1] For some small molecules, the T_1 state has been characterized via high-resolution spectroscopy,[2] providing important benchmarks to evaluate computational techniques. However, spectroscopic data are sparse, because of the difficulty of measuring spin-forbidden $T_1 \leftarrow S_0$ transitions.

Acrolein (CH_2═$CHCH$═O), the simplest conjugated enone, has received close attention in computational studies of triplet states.[3,4] In photochemical dynamics simulations, the twisted $^3(\pi,\pi^*)$ state of acrolein is found to mediate the return to the ground state.[4] The photochemical properties of acrolein have in turn stimulated interest in the triplet states of cyclic enones. Experimental[5] and theoretical[6] investigations of cyclic enones have focused on the influence of structural rigidity on triplet-state lifetimes.

The 2-cyclopenten-1-one molecule (2CP), shown in Figure 1 along with its 5-d_1 and 5,5-d_2 isotopomers, is a simple cyclic enone analogous to acrolein. The ground state of 2CP has been well characterized by infrared spectroscopy[7,8] and the $S_1(n,\pi^*)$ excited state by absorption[9] and by fluorescence excitation.[10] By contrast, the lowest-energy triplet surfaces of 2CP have not been investigated spectroscopically, although the triplet states have been the subject of several recent computational studies,[6,11,12] one of which is reported in the paper that follows this one.[13] The only reported experimental probe is a solution-phase determination of the lowest triplet energy using photoacoustic calorimetry.[14] In this paper, we present the first direct spectroscopic study of 2CP in its lowest triplet (n,π^*) state. We have used the highly sensitive cavity ringdown[15] (CRD) technique to record vibronically resolved absorption spectra of 2CP vapor and its 5,5-d_2 derivative near 385 nm. The very weak ($\epsilon_{max} < 1$ M^{-1} cm^{-1}) absorption band system in this region is due to a spin-forbidden $\pi^* \leftarrow n$ electronic transition originating in the ground state. We designate this transition as $T_1(n,\pi^*) \leftarrow S_0$. Some ambiguity exists as to whether the upper state of the transition is T_1 or T_2, because the ordering of the lowest $^3(n,\pi^*)$ and $^3(\pi,\pi^*)$ states is not known with certainty. However, support for the $T_1(n,\pi^*)$ designation comes from the results of both the

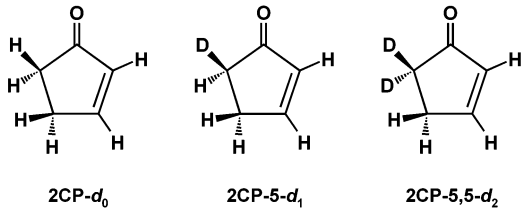

Figure 1. 2-Cyclopenten-1-one (2CP) and its deuterated derivatives investigated in this work.

† Part of the special issue "Charles S. Parmenter Festschrift".

* To whom correspondence should be addressed. E-mail: druckers@uwec.edu.

‡ University of Wisconsin−Eau Claire.

§ Hanyang University.

|| Texas A&M University.

10.1021/jp0304430 CCC: $25.00
Published on Web 10/11/2003

photoacoustic calorimetry experiment[14] (see the Discussion section) and the computational study presented in the next paper.[13]

Our identification of the origin-band frequency in the CRD spectrum offers a precise benchmark for evaluating computed adiabatic excitation energies of the $^3(n,\pi^*)$ state of 2CP. Existing calculations span substantively different theoretical approaches. García-Expósito et al.[6] used the CASSCF procedure to calculate the minima of the $^3(n,\pi^*)$ and $^3(\pi,\pi^*)$ states, as well as their conical intersection. Sunoj et al.[11] calculated vertical and adiabatic excitation energies of the two triplet states using both ab initio (CIS) and density-functional techniques. Froese et al.[12] applied an integrated molecular orbital + molecular mechanics method to calculate triplet-state adiabatic excitation energies for 2CP and larger cyclic systems. Most recently, Choo et al.[13] used a density functional technique to calculate the energy minima as well as fundamental vibrational frequencies for the $^3(n,\pi^*)$ and $^3(\pi,\pi^*)$ states of 2CP. A comparison of calculated and experimental $^3(n,\pi^*)$ excitation energies is presented by Choo et al.[13]

We have assigned about 50 vibronic bands in the CRD spectrum in a region from -500 to $+500$ cm^{-1} relative to the $T_1 \leftarrow S_0$ origin. This has permitted determination of fundamentals for several low-frequency vibrational modes in the T_1 state. For the lowest-frequency mode ν'_{30} (ring-bending, also called ring-puckering), we have determined the first five energy levels in the T_1 state.

In this paper, we place particular emphasis on the ring-bending mode, as its energy-level pattern in the $T_1(n,\pi^*)$ state is found to depart significantly from that of a harmonic oscillator. This behavior was seen previously in the S_0[7,8] and $S_1(n,\pi^*)$[10] states. The ring-bending vibrational mode of 2CP was first investigated in the far-infrared region by Chao and Laane,[7] who found a series of bands between 94 and 116 cm^{-1}. The potential function for this mode was determined and showed the molecule to be planar and relatively rigid in the electronic ground state. Cheatham and Laane reanalyzed the far-infrared spectrum[8] and also investigated the fluorescence excitation spectrum[10] associated with the S_1 state for the -d_0, -d_1, and -d_2 isotopic species. From the far-infrared data, which included ring-bending transitions in the ring-twisting (ν_{29}) excited state, both a refined one-dimensional potential function and a two-dimensional potential-energy surface were determined. The fluorescence excitation data allowed the ring-bending potential function for the S_1 state to be calculated. This showed the molecule to be less rigid in the electronic excited state, resulting from the reduced conjugation.

In the present investigation, we were interested in determining what effect the combination of reduced conjugation and flipping the electron spin would have on the ring-bending potential function and the rigidity of the ring. The CRD data for the $T_1(n,\pi^*)$ state help to answer that question.

Experimental Section

Cavity ringdown spectra were recorded using the pulsed laser system at the University of Wisconsin—Eau Claire. A schematic diagram of the experimental setup is shown in Figure 2. A tuneable dye laser (Lambda Physik ScanMate 2E) is pumped by the third harmonic (355 nm) of a Nd:YAG laser (Continuum Surelite II) operating at 10 Hz. The dyes Exalite 376, 384, and 392A (Exciton) are used to cover the wavelength region from 372 to 395 nm. For medium-resolution scans as conducted in the CRD studies of 2CP, the dye laser is used without its intracavity Etalon, resulting in an output bandwidth of approximately 0.1 cm^{-1}.

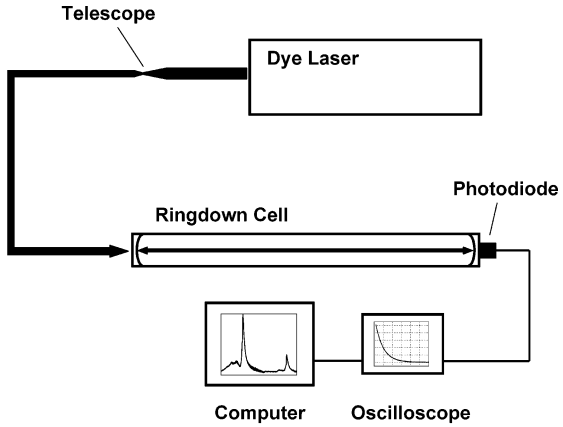

Figure 2. Schematic diagram of the experimental setup used to record cavity ringdown (CRD) spectra.

The dye laser output (typically a few mJ/pulse) is directed through a focusing telescope in order to reduce the beam diameter to about 1 mm. The laser then enters the cavity ringdown sample cell, which is a stainless steel tube 1 m in length, bounded by high-reflectivity concave mirrors (VLOC, quoted $R = 0.999$) with 6-m radii of curvature. The mirrors are vacuum-sealed to the ends of the cell using mirror mounts (Los Gatos Research) equipped with adjustment micrometers. The light exiting the cell is detected by a PIN photodiode (Thorlabs DET 110) that has a 20-ns rise time. The photodiode signal is sent to the 50-ohm input of a digital oscilloscope (Tektronix TDS 3054). An internal 20-MHz filter removes high-frequency components, and the resulting exponential decay signal is captured by the oscilloscope.

The decay traces from typically eight laser pulses are averaged and then uploaded to a computer, where the rate constant is determined (along with amplitude and baseline) using a nonlinear least-squares (Levenberg—Marquardt) routine. The CRD spectrum is recorded as a plot of the decay rate constant k vs wavelength.

Wavelength calibration is accomplished by using the opto-galvanic signal from argon in a hollow-cathode lamp. The wavelength accuracy of sharp, unblended features in the CRD spectra is estimated to be ± 0.001 nm (0.07 cm^{-1}).

2-Cyclopenten-1-one was obtained from Acros and used without further purification. The 5,5-d_2 derivative was prepared as described by Chao and Laane.[7] Because this preparation also yields a few percent of the 5-d_1 isotopomer, several of the spectroscopic bands for that species could also be observed. To record a CRD spectrum, the cell was initially filled with 2CP at its room-temperature vapor pressure of 2 Torr. After a few hours, the cell pressure typically dropped to 1.6 Torr due to adsorption of 2CP onto the stainless steel cell walls.

CRD spectra of 2CP-d_0 are shown in Figures 3—6. In these figures, the CRD spectrum of the evacuated cell has been subtracted to eliminate the effect of changing mirror reflectivity on the baseline. Because the mirror reflectivity is a very smooth function of wavelength, it was possible to substitute the recorded empty-cell spectrum with a noiseless one generated by using a high-order polynomial fit. Subtraction of the empty-cell spectrum has permitted determination of the fractional photon loss due to molecular absorption. The fractional loss per pass through the cell is $(\Delta k)l/c$,[15] where Δk is the CRD decay constant with empty-cell value subtracted, l is the length of the cell, and c is the speed of light. The CRD spectrum in Figure 3 indicates the fractional photon loss, as well as the molar extinction coefficient that follows from application of Beer's law.

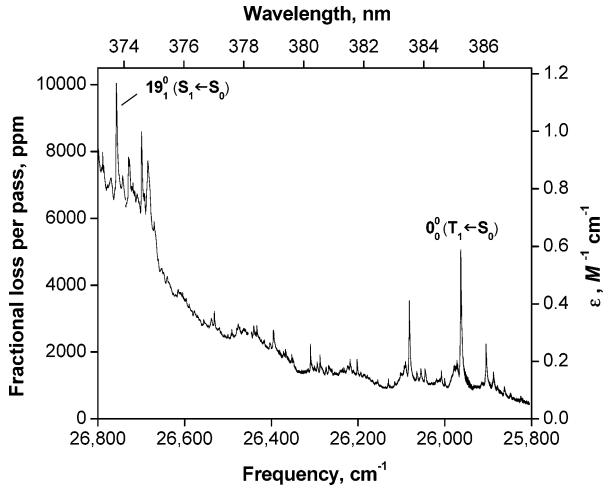

Figure 3. Room-temperature CRD spectrum of 2CP vapor (1.6 Torr), showing the $T_1 \leftarrow S_0$ origin band near 385 nm, as well as the onset of $S_1 \leftarrow S_0$ transitions near 375 nm. This spectrum is a composite of several single scans recorded over adjacent wavelength regions. The wavelength increment within a scan was 0.001 nm. The empty-cell spectrum (simulated by a polynomial fit; see text) has been subtracted.

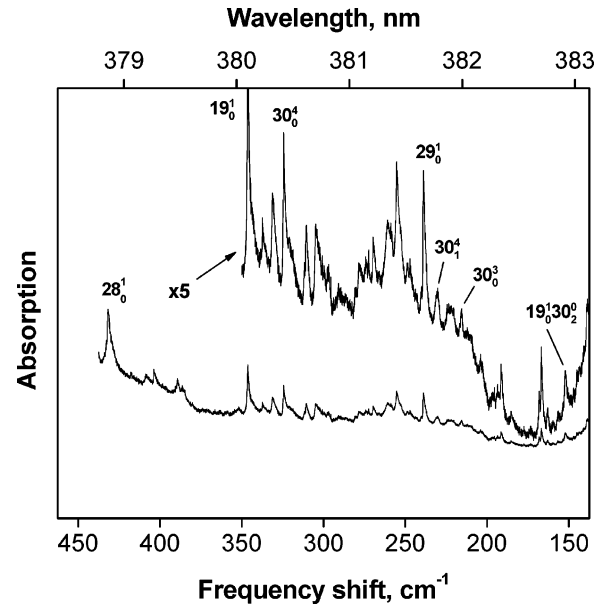

Figure 4. CRD spectrum of 2CP (1.6 Torr), showing vibronic assignments of the $T_1 \leftarrow S_0$ band system in a region to high wavenumber of the origin band. This spectrum was obtained by subtracting the simulated empty-cell spectrum from the average of two sample scans. The wavelength increment was 0.001 nm. The upper trace has been vertically displaced after expansion by a factor of 5.

The signal-to-noise ratio of the $T_1 \leftarrow S_0$ origin band is approximately 250. For the weakest detectable assigned absorption band (19_1^0; see inset of Figure 6), the fractional photon loss per pass through the CRD cell is about 50 ppm. Off-resonance noise in the CRD spectra is due predominantly to mode-beating that is evident in the ringdown decay curves. The mode-beating could in principle be eliminated by installation of a spatial-filtering pinhole at the focus of the beam-reducing telescope.

Results and Discussion

Vibronic Assignments. Figure 3 shows the CRD spectrum of 2CP-d_0 vapor in a 1000-cm^{-1} region that includes the 385-nm origin band of the $T_1 \leftarrow S_0$ system. The region shown

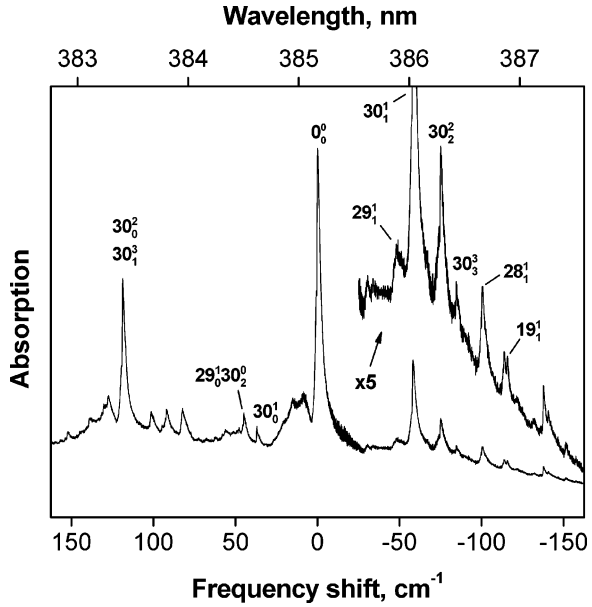

Figure 5. Continuation of the spectrum of Figure 4, showing vibronic assignments in the region of the $T_1 \leftarrow S_0$ origin band. Vertical displacement of upper (expanded) trace is different from that of Figure 4.

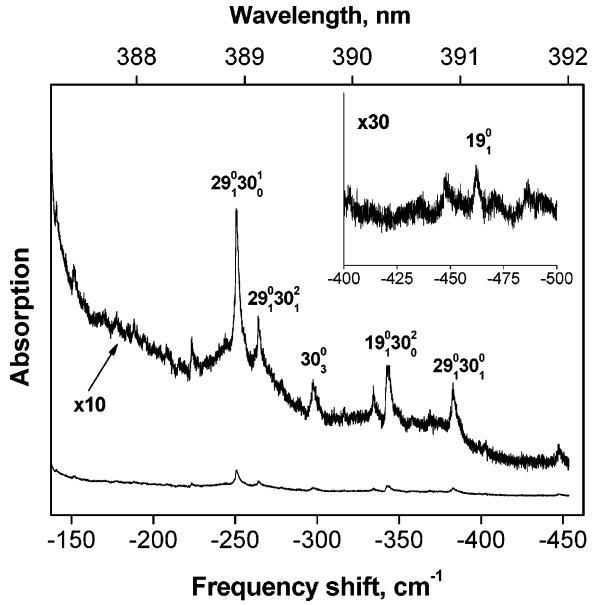

Figure 6. Continuation of the spectrum of Figure 5, showing vibronic assignments in a region to low wavenumber of the $T_1 \leftarrow S_0$ origin band. Vertical displacements of expanded traces are different from that of Figure 5.

extends to about 27 000 cm^{-1} and approaches the $S_1 \leftarrow S_0$ origin at 27 210 cm^{-1}.[10] Several relatively intense bands are observed at the extreme blue end of the CRD spectrum, one of which has been previously assigned[9] as the $S_1 \leftarrow S_0$ 19_1^0 transition (−464 cm^{-1} relative to the singlet origin).

The most intense transition in the red end of the CRD spectrum, observed at ($d_0/d_1/d_2$) 25 963.55(7)/25 959.38(7)/25 956.18(7) cm^{-1}, is assigned as the $T_1 \leftarrow S_0$ origin band. This assignment is based in part on a comparison to the band intensities in the $S_1 \leftarrow S_0$ spectrum.[9,10] The $S_1 \leftarrow S_0$ origin band has a large Franck−Condon factor, because the molecule remains planar following excitation. (By contrast, nonconjugated enones undergo pyramidalization at the carbonyl carbon.) For 2CP, several recent computational studies predict the lowest

triplet states to be planar[6,11] or nearly planar.[13] Thus, the $T_1 \leftarrow S_0$ origin band is expected to be most intense, as in the singlet case.

We assign the upper electronic state in the CRD spectrum as $^3(n,\pi^*)$, though the $^3(n,\pi^*)$ and $^3(\pi,\pi^*)$ states of 2CP are predicted[6,11-13] to be nearly isoenergetic. Our electronic assignment is based on observed vibronic band intensities. For the origin band, the molar extinction coefficient extracted from the CRD decay constant is 0.59 $M^{-1}cm^{-1}$. This value is typical of singlet−triplet transitions involving $\pi^* \leftarrow n$ excitation.[16] The observed ϵ_{max} is several orders of magnitude greater than that expected for spin-forbidden $\pi^* \leftarrow \pi$ transitions.[16] Such transitions would lie just at the detectability limit of our experiment as it is currently constructed. The vibronic bands assigned below are thus assumed to be part of the $\pi^* \leftarrow n$ system, but it is possible that some very weak, unassigned bands are $\pi^* \leftarrow \pi$ transitions.

Table 1 lists assigned vibronic transitions of the 2CP-d_0 and -d_2 isotopomers. These bands occur in a region from −500 to +500 cm^{-1}, relative to the d_0/d_2 origin. Expanded views within this region of the CRD spectrum are shown in Figures 4−6. At wavenumbers greater than +500 cm^{-1}, hot bands of the $S_1 \leftarrow S_0$ transition cause some ambiguities in the assignment process. This interference is discussed in more detail at the end of this section.

The low-energy region of the CRD spectrum (to the red of the $T_1 \leftarrow S_0$ origin band), shown in Figures 5 and 6, provides a starting point for establishing the assignments. This is the least congested portion of the spectrum, because it contains only hot bands that are associated with low-frequency vibrational modes. Low-frequency modes of 2CP are ν_{30} (ring-bending), ν_{29} (ring-twisting), ν_{28} (out-of-plane carbonyl deformation), and ν_{19} (in-plane carbonyl deformation). The first three of these are of a″ symmetry and are subject to a Δv = even selection rule. This symmetry restriction further simplifies the spectrum and has facilitated some of the assignments discussed below.

Attached to the origin band is a $\Delta v = 0$ sequence in ν_{30}. For the -d_0 isotopomer, the 30_1^1, 30_2^2, and 30_3^3 transitions are observed at −58.3, −75.1, and −84.6 cm^{-1}, respectively. These assignments were established via observation of additional bands related to the sequence members by precisely known[8] ν_{30} ground-state combination differences. For example, starting with the band at −75.1 cm^{-1} assigned as 30_2^2, and knowing the energy separation (194.1 cm^{-1}) between $v'' = 0$ and $v'' = 2$, one expects the 30_0^2 transition to occur at −75.1 + 194.1 = +119.0 cm^{-1}. The expected transition is observed at +118.7 cm^{-1}, corroborating the $v' = 2$ energy. The 30_1^1 and 30_3^3 sequence members likewise successfully predict additional transitions having $v' = 1$ and 3. Although the 30_4^4 sequence member is not detectable, three other bands having $v' = 4$ are observed. For $v' = 5$, the only assigned band is the 30_1^5 transition. The inferred $v' = 5$ energy is in accord with the ring-bending potential-energy function (see next section) determined from the other four levels.

The $v' = 1-5$ level energies, determined from the bands involving ν'_{30}, are listed in Table 2. Typically, all observed bands with a given value of v'_{30} were used to determine the best-fitting energy of that level. In a few cases of broad or overlapped bands, the uncertainty in the position of the maximum significantly exceeded the wavelength uncertainty of the laser system. Such bands were excluded from the fit of ν'_{30} level energies.

Further support for the ν'_{30} band assignments comes from our observation of the $\Delta v_{30} = 0$ sequence in the CRD spectrum of 2CP-d_2. Figure 7 shows these sequence members in a region near the -d_2 origin band. As in the case of the -d_0 isotopomer, these transitions predict additional bands having the same value of v'_{30}. The ν'_{30} energy levels determined for the -d_2 species are listed in Table 2. These levels show isotope shifts that are consistent with ν_{30} level shifts observed in both the ground[8] and S_1[10] states.

In the -d_2 spectrum, the origin as well as the ν_{30} sequence bands are accompanied by weak satellites or shoulders attributable to -d_1 isotopic contamination. To confirm the assignment of -d_1 bands, we prepared some deuterated samples of 2CP with up to 10% H_2O added to the reaction mixtures. These modified products contain appreciable percentages of 2CP-d_1 (confirmed by nmr) in addition to -d_2. The CRD spectra of the modified products are plotted in Figure 7 along with the original 2CP-d_2 spectrum. The shoulders evident in the original spectrum appear

TABLE 1: CRD Transition Frequencies[a] (cm^{-1}) and Assignments for 2-Cyclopenten-1-one-d_0 and -d_2

2CP-d_0		2CP-d_2		
obs.	calc.[b]	obs.	calc.	assignment
−462.0	−464	−446.8	−449	19_1^0
−403.0	−405.5			30_4^0
−382.8	−383.1	−369.7	*c*	$29_1^0 30_1^0$
−368.9	−369.0			30_4^1
−343.3	−345	−345.4	−347	$19_1^0 30_0^2$
−297.4	−298.2			30_3^0
−288.2	−286.8	−281.6	−280.7	29_1^0
−288.2	−286.6			30_4^2
−264.0	−264.2	−267.5	*c*	$29_1^0 30_1^2$
−250.4	−250.3	−251.1	−251.0	$29_1^0 30_0^1$
−194.1	−194.1	−174.2	−174.6	30_2^0
−157.5	−157.6			30_2^1
−115.8	−118	−116.2	−119	19_1^1
−100.4	−100	−94.5	*d*	28_1^1
−84.6	−84.5	−83.3	−83.1	30_3^3
−75.1	−75.2	−72.7	−72.7	30_2^2
−58.3	−57.9	−55.2	−55.2	30_1^1
−48.0	−47.9			29_1^1
0.0	0.0	0.0	0.0	0_0^0
21.2	19.6			30_2^3
37.0	36.5			30_0^1
44.8	44.8	53.3	53.2	$29_0^1 30_2^0$
48.2	48.0			$19_0^1 30_3^0$
62.3	61.9			$29_0^1 30_3^2$
82.4	84.0			$29_0^1 30_2^1$
118.7	118.9	101.8	101.9	30_0^2
119.4	119.3	100.0	99.9	30_1^3
130.3	130.4	104.0	105.9	30_2^4
		117.5	117.7	30_3^5
143.7	144.5	141.5	142.9	$29_0^1 30_1^0$
152.1	152.1			$19_0^1 30_2^0$
159.8	159.6			$29_1^0 30_0^5$
185.2	183.7			$29_0^1 30_1^1$
215.6	213.7	186.4	184.8	30_0^3
230.2	230.1			30_1^4
238.9	238.9	227.6	227.8	29_0^1
		245.0	245.3	$19_0^1 30_1^0$
		245.0	245.7	$28_0^1 30_2^0$
266.0	265.7			$29_0^1 30_1^2$
278.2	278.1	258.1	258.1	$29_0^1 30_0^1$
324.5	324.5	280.5	280.5	30_0^4
337.3	337.4	335.8	335.4	$28_0^1 30_1^0$
346.2	346.2	330.4	330.2	19_0^1
351.8	352.0	300.9	300.7	30_1^5
359.5	360.1	335.8	335.8	$29_0^1 30_0^2$
431.8	431.8	420.4	420.3	28_0^1

[a] Frequencies are relative to the electronic origin at 25 963.55 and 25 956.18 cm^{-1}, respectively, for 2CP-d_0 and 2CP-5,5-d_2. [b] Calculated from other observed ground[8] and excited-state vibrational frequencies and the assignments in this work. [c] The ground-state vibrational frequency was not previously determined. [d] The 28_1^1 transition frequency (−94.5 cm^{-1}), taken together with the 28_0^1 frequency (observed at 420.4 cm^{-1}), implies a ground-state ν_{28} fundamental of 514.9 cm^{-1} for 2CP-d_2. The ν_{28} fundamental frequency for this isotopomer was not available in previous[8] infrared studies.

TABLE 2: Observed and Calculated $T_1(n,\pi^*)$ Energy Levels for the Ring-Bending Vibrational Mode of 2-Cyclopenten-1-one Isotopomers

	2CP-d_0			2CP-d_1			2CP-d_2		
ring-bending level (ν'_{30})	obs.[a]	calc.I[b]	calc. II[b]	obs.	calc. I	calc. II	obs.	calc. I	calc. II
1	36.5	35.7	35.7	32.8	32.5	32.4	29.7	29.5	29.5
2	118.9	119.6	119.6	109.2	110.5	110.5	101.9	102.7	102.7
3	213.7	214.4	214.4	199.1	198.4	198.4	184.8	184.7	184.7
4	324.5	324.3	324.4				280.5	280.1	280.2
5	446.4	445.7	445.7				385.6	385.7	385.7

[a] Determined from the set of observed transitions terminating in ν'_{30}. [b] Calc. I: rocking parameter $R = 0$; Calc. II: rocking parameter $R = 1.1$.

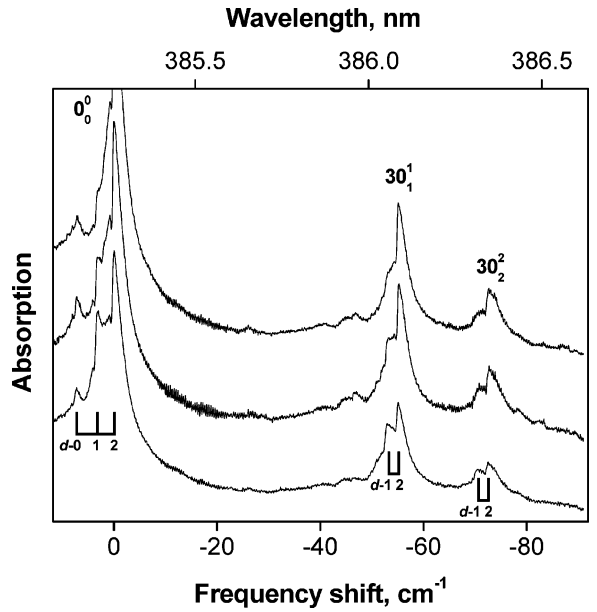

Figure 7. CRD spectra of deuterated samples of 2CP. Upper trace: sample prepared using D_2O and D_2SO_4, according to the procedure of Chao and Laane.[7] This yields predominantly 2CP-d_2. Middle and lower traces: samples prepared with 2% and 10% H_2O, respectively, added to the reaction mixture. Transitions due to 2CP-d_1 become distinguishable in the middle and lower spectra.

in the modified product spectra as distinguishable peaks, assignable to 2CP-d_1. For the -d_1 isotopomer, the 30_1^1, 30_2^2, and 30_3^3 bands are observed at -56.2, -73.7, and -81.4 cm^{-1}, respectively, relative to the -d_1 origin. These band positions, together with known ground-state combination differences[8] for 2CP-d_1, were used to determine the ν'_{30} energies listed in Table 2. The isotope shifts are consistent with those found for the -d_2 isotopomer.

In the CRD spectrum of 2CP-d_0, the 30_1^0 band is expected at -94.4 cm^{-1}, based on the known ground-state fundamental frequency of ν_{30}. The 30_1^0 band is not observed, nor are some others in which Δv_{30} is odd. The Franck−Condon factors for such transitions vanish because of the a″ symmetry of the ring-bending mode. In the $S_1 \leftarrow S_0$ (A″ ← A′) absorption band system, some of the transitions with $\Delta v_{30} =$ odd (including 30_1^0 and 30_0^1) are made weakly allowed by vibronic interaction involving singlet states of A′ symmetry. The $^3(n,\pi^*)$ state, with a possibility of both A′ and A″ spin−orbital symmetries, apparently does not undergo the required vibronic interaction as extensively as the $^1(n,\pi^*)$ state does.

Another low-frequency out-of-plane (a″) mode is ν_{29}, ring-twisting. Several symmetry-allowed transitions involving ν_{29} are observed in the CRD spectra. One is $29_1^0 30_0^1$, at (d_0/d_2) $-250.4/-251.1$ cm^{-1}. The expected position of this band is $-250.7/-251.0$ cm^{-1}, based on the precisely known ν''_{29} fundamental frequency,[8] combined with the ν'_{30} fundamental derived from the observed 30_1^1 transition. The very good agreement between the observed and expected $29_1^0 30_0^1$ band position adds support for the assignment of the 30_1^1 and origin bands.

In addition to the ν'_{30} level energies, the fundamental frequencies ν'_{29}, ν'_{28}, and ν'_{19} have been established in this work. The frequencies were determined through observation of both the N_0^1 and N_1^1 bands for $N = 29$, 28, and 19. These bands are listed in Table 1 for the -d_0 isotopomer. The assignments are verified via calculation of the $N_0^1 - N_1^1$ combination differences, which should predict ground-state fundamental frequencies. The combination differences are $238.9 - (-48.0) = 286.9$ cm^{-1}; $431.8 - (-100.4) = 532.2$ cm^{-1}; $346.2 - (-115.8) = 462.0$ cm^{-1}; respectively, for ν_{29}, ν_{28}, and ν_{19}. These values agree well with the measured ground-state fundamentals 286.8,[8] 532,[7] and 464 cm^{-1}.[7]

For ν_{19}, the measured ground-state fundamental (from infrared studies) is slightly greater than the value inferred from the 19_0^1 and 19_1^1 CRD band positions. However, support for the 19_0^1 and 19_1^1 assignments comes from our observation of a band at -462.0 cm^{-1}, which we assign as 19_1^0. This assignment implies a ν_{19} fundamental that agrees precisely with the $19_0^1 - 19_1^1$ combination difference. The disagreement with the infrared value of 464 cm^{-1} may be traced to rotational branch structure. In the room-temperature infrared spectrum, *P* and *R* branch heads are observed at 458 and 471 cm^{-1}, respectively.[7] The 464 cm^{-1} value is that reported for the band center. Rotational branch structure is likely different in the $T_1 \leftarrow S_0$ CRD spectrum. Moreover, we report band maxima observed in the CRD spectrum rather than centers. Hence, a 2-cm^{-1} discrepancy in frequency is not unreasonable. A discrepancy of the same magnitude and direction occurs for the -d_2 isotopomer.

The region of the CRD spectrum greater than $+500$ cm^{-1} shows further band structure, but superimposed on a steeply sloped baseline. This is seen in Figure 3. The baseline behavior at high wavenumber is likely due to (1) the increasing density of triplet vibrational states and (2) the onset of hot bands associated with the $S_1 \leftarrow S_0$ transition. The 19_1^0 transition of the singlet system is observed near 375 nm.[9] Other features in the 375-nm region are not assigned in the present work because they could be either $S_1 \leftarrow S_0$ hot-band or $T_1 \leftarrow S_0$ cold-band transitions. In particular, it is not possible to determine the ν'_5 (carbonyl stretch) or ν'_6 (C=C stretch) fundamentals of the triplet state, because the 5_0^1 and 6_0^1 bands would be submerged by tremendously intense (by comparison) $S_1 \leftarrow S_0$ bands near the 368-nm singlet origin.

Ring-Bending Potential-Energy Function. We have used the ring-bending (ν'_{30}) energy levels obtained from the CRD spectra to determine a one-dimensional potential-energy function for this vibrational mode. As in the previous one-dimensional studies on the ground[7,8] and S_1 excited-state[10] state potential-energy functions, the vibrational Hamiltonian for the ring bending was selected to have the form

$$H(x) = (-\hbar^2/2)\, \mathrm{d/d}x\, g_{44}(x)\, \mathrm{d/d}x + V(x) \quad (1)$$

where x is the ring-bending coordinate,[7,8,17] $g_{44}(x)$ is the coordinate-dependent kinetic-energy (reciprocal reduced mass) expansion, and $V(x)$ is the potential energy given by

$$V(x) = ax^4 + bx^2 \quad (2)$$

The kinetic-energy expansion was calculated based on vectorial methods previously described[17] using the bond distances and angles calculated in the paper that follows by Choo et al.[13] Both the standard bisector model and a model allowing rocking of the CH_2 group adjacent to the carbonyl group were utilized. A rocking parameter[17] of 1.1 was found to predict best the observed isotopic shifts for the bending vibration. This corresponds to a rocking angle of approximately 3° when the dihedral angle of bending is 12°. For the S_0 and S_1 states, a rocking parameter of 0.67 best fits the isotopic data. Table 3 lists the reduced masses and kinetic-energy coefficients for both the no rocking ($R = 0$) and rocking ($R = 1.1$) models for all three isotopic species of interest.

Table 2 and Figure 8 show the ring-bending energy levels determined from the spectra for the $T_1(n,\pi^*)$ states of the -d_0, -d_1, and -d_2 isotopomers of 2CP. These data were used to determine the potential-energy parameters a and b in eq 2 for each isotope and for both the $R = 0$ and 1.1 models. The results are shown in Tables 2 and 4. The agreement between observed and calculated frequencies can be seen to be excellent, as the average deviation is less than 0.6 cm^{-1}. The calculated barriers to planarity for the six calculations range from 42.0 to 43.5 cm^{-1}, so the value can safely be taken to be 43 $\pm$1 cm^{-1}. Figure 9 shows the T_1 potential-energy function and energy separations for the $R = 1.1$ calculation for the -d_0 isotopomer. The energy minima are at $x = \pm 0.055$ Å, which correspond to dihedral angles of $\pm$12°.

Figure 10 compares the one-dimensional ring-bending potential functions for the S_0, S_1, and T_1 electronic states. As expected, the electronic excitation to an antibonding orbital reduces the conjugation and results in a less rigid ring. The molecule in the S_1 state becomes more floppy but remains planar. However, in the triplet state, the molecule bends into a puckered structure with energy minima at $\pm$12°. This observation is consistent with the general proclivity for "looseness"[18] exhibited by triplet states due to repulsion between electrons that are required to be in separate orbitals.

Ordering of (n,π^*) and (π,π^*) Triplet States. The present work, combined with the results of a photoacoustic calorimetry (PAC) experiment,[14] addresses the question of the ordering of the two lowest triplet states. The PAC experiment involved excitation of 2CP at 355 nm (an energy above that of the S_1 origin) in cyclohexane solution, followed by measurement of acoustic waves generated by the 2CP in its "relaxed" triplet state. The relaxed triplet state in solution presumably corresponds to the lowest vibronic level in the triplet manifold. The relaxed triplet state would be reached by the molecule after undergoing $S_1 \rightsquigarrow$ triplet intersystem crossing and then solvent-induced vibrational relaxation.

The PAC experiment established the energy of the relaxed triplet state of 2CP in cyclohexane solution to be 73.1 $\pm$ 1.1 kcal/mol.[14] This value may be compared with the excitation energy of the $^3(n,\pi^*)$ state determined in the present vapor-phase CRD work. The origin-band wavenumber of 25 964 cm^{-1} corresponds to 74.23 kcal/mol. This value is just at the upper uncertainty limit of the PAC measurement of the relaxed triplet energy. Of course, the stated uncertainty limits are blurred somewhat in this comparison, because the cyclohexane solvent would very likely shift the S_0-triplet energy gap from its vapor-phase value. We conclude that the present CRD measurements are entirely consistent with the relaxed triplet state having an (n,π^*) electronic label; viz. the $^3(n,\pi^*)$ state is lower than the $^3(\pi,\pi^*)$ state.

If the ordering were the other way around, then the origin of the triplet $\pi^* \leftarrow \pi$ transition would have to be located in the region between 25 964 and about 25 200 cm^{-1} to be consistent with the PAC measurement of the relaxed triplet energy. We

TABLE 3: Reduced Masses (a.u.) and Kinetic-Energy Coefficients[a] for the $T_1(n,\pi^*)$ Ring-Bending Vibrational Mode of 2-Cyclopenten-1-one Isotopomers

calc.[b]	μ	$g_{44}^{(0)}$	$g_{44}^{(1)}$	$g_{44}^{(2)}$	$g_{44}^{(3)}$	$g_{44}^{(4)}$	$g_{44}^{(5)}$	$g_{44}^{(6)}$
2CP-d_0								
I	247	4.048	0.0	6.403	0.0	−72.52	0.0	−96.19
II	272	3.681	0.0	5.312	0.0	−62.81	0.0	−74.29
2CP-d_1								
I	269	3.723	0.0	4.959	0.0	−65.01	0.0	−79.60
II	303	3.297	0.0	3.795	0.0	−53.38	0.0	−59.03
2CP-d_2								
I	287	3.479	0.0	3.775	0.0	−58.24	0.0	−70.69
II	331	3.020	0.0	2.591	0.0	−45.33	0.0	−52.50

[a] The form of the kinetic-energy expansion is $g_{44}(x) = \sum_{k=0}^{6} g_{44}^{(k)} x^k$. The subscripts $i = 1-3$ for g_{ii} are reserved for the molecular rotations. The given coefficients are multiplied by 10^3 in units of μ^{-1} Å^{-k}. [b] Calc. I: rocking parameter $R = 0$; Calc. II: rocking parameter $R = 1.1$.

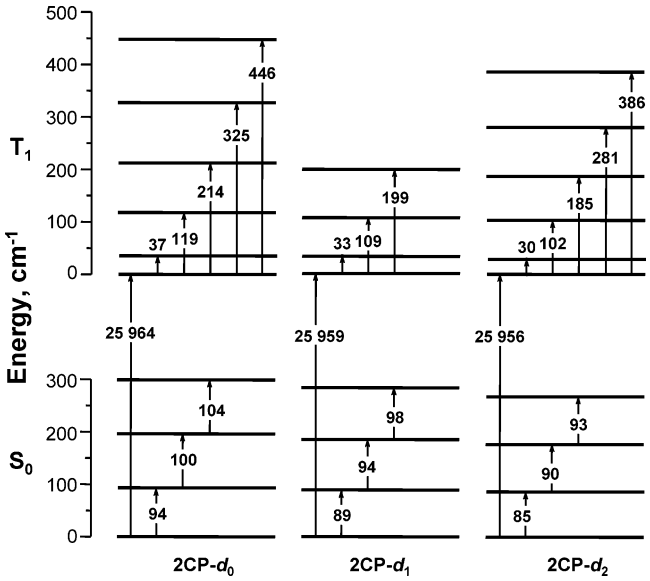

Figure 8. Energy-level diagram, determined from the present vibronic assignments (triplet state) and previous[8] far-infrared results (ground state), for the ring-bending vibrational mode of 2CP-d_0, 2CP-d_1, and 2CP-d_2.

TABLE 4: Potential-Energy Parameters[a] for the Ring-Bending Vibrational Mode of 2-Cyclopenten-1-one Isotopomers in the $T_1(n,\pi^*)$ Electronic State

calc.[b]	a, cm^{-1} Å^{-4}	b, cm^{-1} Å^{-2}	barrier, cm^{-1}
2CP-d_0			
I	4.695×10^6	-2.858×10^4	43.5
II	5.693×10^6	-3.149×10^4	43.5
2CP-d_1			
I	4.507×10^6	-2.761×10^4	42.3
II	5.764×10^6	-3.129×10^4	42.5
2CP-d_2			
I	4.296×10^6	-2.688×10^4	42.0
II	5.718×10^6	-3.103×10^4	42.1

[a] The potential-energy function is $V(x) = ax^4 + bx^2$. [b] Calc. I: rocking parameter $R = 0$; Calc. II: rocking parameter $R = 1.1$.

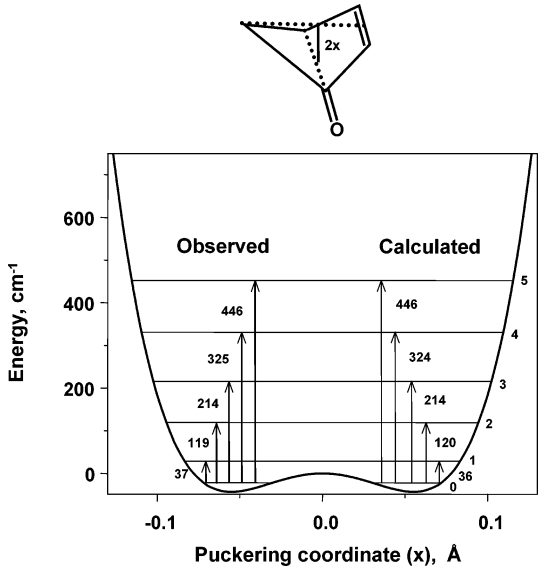

Figure 9. Ring-bending potential-energy function for the $T_1(n,\pi^*)$ state of 2CP. This function was fit to the observed ring-bending levels of the $-d_0$ isotopomer, using a rocking parameter of 1.1.

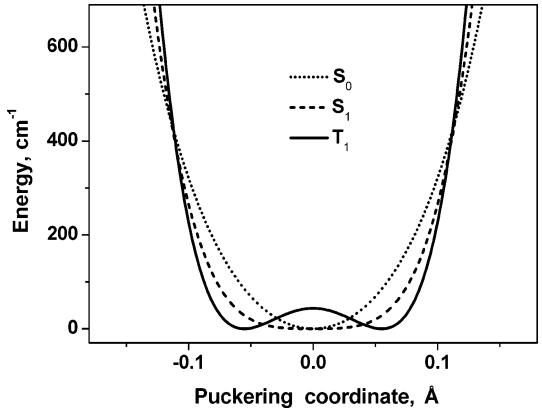

Figure 10. Comparison of experimentally determined ring-bending potential-energy functions for the S_0, $T_1(n,\pi^*)$, and $S_1(n,\pi^*)$ states of 2CP.

regard this scenario as unlikely, considering we detected no transitions at wavenumber lower than 25 400 cm^{-1}, and nearly every CRD band at higher wavenumber than this has been assigned to the $\pi^* \leftarrow n$ triplet system.

Conclusions

In this work, we used cavity ringdown spectroscopy to characterize the $T_1(n,\pi^*)$ state of 2-cyclopenten-1-one and deuterated derivatives. We have recorded the first $T_1 \leftarrow S_0$ absorption spectrum of 2CP vapor and assigned nearly 50 vibronic bands. Vibronic analysis has permitted determination of several low-frequency fundamentals in the $T_1(n,\pi^*)$ state. In addition, we have determined the five lowest energy levels in the very anharmonic ring-bending mode for the $T_1(n,\pi^*)$ state and used these levels to fit a one-dimensional potential-energy function for ring bending. The potential-energy function has a double minimum with equivalent, slightly puckered equilibrium geometries and a small (43 cm^{-1}) barrier to planarity. This is in subtle contrast to the S_1 state, which was found previously[10] to have a planar, yet still flexible structure.

The T_1 and S_1 states, with the same nominal (n,π^*) electronic configuration, both show an enhanced tendency toward non-planarity as a consequence of the reduced conjugation. The effect is more pronounced for T_1, which is observed to have a slightly puckered equilibrium geometry. The slight difference observed between the $S_1(n,\pi^*)$ and $T_1(n,\pi^*)$ ring-puckering potentials may plausibly be traced to configuration mixing within distinctly different manifolds of excited spin−orbital states.

Acknowledgment is made by S.D. to the donors of the Petroleum Research Fund (33947-GB6), administered by the American Chemical Society, for partial support of this research. S.D. also gratefully acknowledges funding from the Research Corporation (CC4938), The Camille and Henry Dreyfus Foundation, Inc. (Faculty Start-up Grant for Undergraduate Institutions), and the Office of Research and Sponsored Programs of the University of Wisconsin—Eau Claire, as well as a gift of equipment from Prof. Robert Field. J.C. thanks the Korean Science and Engineering Foundation (Grant Number R14-2002-004-01000) for financial support. J.L. thanks the National Science Foundation and Robert A. Welch Foundation for financial support.

References and Notes

(1) See, for example: (a) Chesnut, D. B. *J. Comput. Chem.* **2001**, *22*, 1702. (b) Woeller, M.; Grimme, S.; Peyerimhoff, S. D.; Danovich, D.; Fiylatov, M.; Shaik, S. *J. Phys. Chem. A* **2000**, *104*, 5366. (c) Brink, M.; Jonson, H.; Ottosson, C.-H. *J. Phys. Chem. A* **1998**, *102*, 6513. (d) Stanton, J. F.; Gauss, J. *Spectrochim. Acta Part A* **1997**, *53*, 1153. (e) Yamaguchi, Y.; Wesolowski, S. S.; Van Huis, T. J.; Schaefer, H. F. *J. Chem. Phys.* **1998**, *108*, 5281. (f) Scheiner, S. *J. Phys. Chem. A* **2000**, *104*, 5898. (g) Mebel, A. M.; Luna, A.; Lin, M. C.; Morokuma, K. *J. Chem. Phys.* **1996**, *105*, 6439.

(2) See, for example: (a) Ottinger, C.; Winkler, T *Chem. Phys. Lett.* **1999**, *314*, 411. (b) Robinson, A. G.; Winter, P. R.; Zwier, T. S. *J. Chem. Phys.* **2002**, *116*, 7918. (c) Liu, H.; Lim, E. C.; Muñoz-Caro, C.; Niño, A.; Judge, R. H.; Moule, D. C. *J. Chem. Phys.* **1996**, *105*, 2547. (d) Tomer, J. L.; Holtzclaw, K. W.; Pratt, D. W.; Spangler, L. H. *J. Chem. Phys.* **1988**, *88*, 1528. (e) Moule, D. C.; Sharp, A. C.; Judge, R. H.; Liu, H.; Lim, E. C. *J. Chem. Phys.* **1998**, *108*, 1874. (f) Ottinger, C.; Vilesov, A. F.; Winkler, T *Chem. Phys. Lett.* **1993**, *208*, 299.

(3) (a) Fang, W.-H. *J. Am. Chem. Soc.* **1999**, *121*, 8376. (b) Fang, W.-H. *Chem. Phys. Lett.* **2000**, *325*, 683. (c) Broeker, J. L.; Eksterowicz, J. E.; Belk, A. J.; Houk, K. N. *J. Am. Chem. Soc.* **1995**, *117*, 1847. (d) Wilsey, S.; González, L.; Robb, M. A.; Houk, K. N. *J. Am. Chem. Soc.* **2000**, *122*, 5866.

(4) (a) Reguero, M.; Olivucci, M.; Bernardi, F.; Robb, M. A. *J. Am. Chem. Soc.* **1994**, *116*, 2103. (b) Bernardi, F.; Olivucci, M.; Robb, M. A. *Pure Appl. Chem.* **1995**, *67*, 17.

(5) (a) Bonneau, R. *J. Am. Chem. Soc.* **1980**, *102*, 3816. (b) Schuster, D. I.; Woning, J.; Kaprinidis, N. A.; Pan, Y.; Cai, B.; Barra, M.; Rhodes, C. A. *J. Am. Chem. Soc.* **1992**, *114*, 7029. (c) Schuster, D. I.; Dunn, D. A.; Heibel, G. E.; Brown, P. B.; Rao, J. M.; Woning, J.; Bonneau, R. *J. Am. Chem. Soc.* **1991**, *113*, 6245.

(6) García-Expósito, E.; Bearpark, M. J.; Ortuño, R. M.; Branchadell, V.; Robb, M. A.; Wilsey, S. *J. Org. Chem.* **2001**, *66*, 8811.

(7) Chao, T. H.; Laane, J. *J. Mol. Spectrosc.* **1973**, *48*, 266.

(8) Cheatham, C. M.; Laane, J. *J. Chem. Phys.* **1991**, *94*, 5394.

(9) Gordon, R. D.; Orr, D. R. *J. Mol. Spectrosc.* **1988**, *129*, 24.

(10) Cheatham, C. M.; Laane, J. *J. Chem. Phys.* **1991**, *94*, 7734.

(11) Sunoj, R. B.; Lakshminarasimhan, P.; Ramamurthy, V.; Chandrasekhar, J. *J. Comput. Chem.* **2001**, *22*, 1598.

(12) Froese, R. D. J.; Morokuma, K. *Chem. Phys. Lett.* **1996**, *263*, 393.

(13) Choo, J. B.; Kim, S.; Drucker, S.; Laane, J. *J. Phys. Chem. A* **2003**, *107*, 10655.

(14) Arnaut, L. G.; Caldwell, R. A.; Elbert, J. E.; Melton, L. A. *Rev. Sci. Instrum.* **1992**, *63*, 5381.

(15) (a) O'Keefe, A.; Deacon, D. A. G. *Rev. Sci. Instrum.* **1988**, *59*, 2544. (b) Scherer, J. J.; Paul, J. B.; O'Keefe, A.; Saykally, R. J. *Chem. Rev.* **1997**, *97*, 25.

(16) Turro, N. J. *Modern Molecular Photochemistry*; University Science Books: Mill Valley, CA, 1991; p 105.

(17) Schmude, R. W.; Harthcock, M. A.; Kelly, M. B.; Laane, J. *J. Mol. Spectrosc.* **1987**, *124*, 369.

(18) Klessinger, M.; Michl, J. *Excited States and Photochemistry of Organic Molecules*; VCH Publishers: New York, 1995.